



A Continuous Multi-material Toolpath Planning for Tissue Scaffolds with Hollowed Features

Ibrahim T. Ozbolat¹ and Bahattin Koc²

¹The University of Iowa, ibrahim-ozbolat@uiowa.edu

²Sabanci University, University at Buffalo bahattinkoc@sabanciuniv.edu

ABSTRACT

This paper presents a new multi-material based toolpath planning methodology for porous tissue scaffolds with multiple hollowed features. Ruled surface with hollowed features generated in our earlier work is used to develop toolpath planning. Ruling lines are reoriented to enable continuous and uniform size multi-material printing through them in two steps. Firstly, all ruling lines are matched and connected to eliminate start and stops during printing. Then, regions with high number of ruling lines are relaxed using a relaxation technique to eliminate over deposition. A novel layer-by-layer deposition process is progressed in two consecutive layers: The first layer with hollow shape based zigzag pattern and the next layer with spiral pattern deposition. Heterogeneous material properties are mapped based on the parametric distances from the hollow features.

Keywords: Solid Freeform Fabrication, Toolpath Planning, Tissue Scaffolds, Multi-material Printing

DOI: 10.3722/cadaps.2010.xxx-yyy

1 INTRODUCTION

Solid Freeform Fabrication (SFF) systems, also known as rapid prototyping systems, make a physical prototype from its computer model, which will be tessellated, sliced and then built layer by layer. SFF has great potential to fabricate heterogeneous objects with complex geometries. Recently, SFF have been widely used in fabrication of biomedical related heterogeneous products such as orthopedic implants [1], tissue scaffolds [2-3] and drug delivery devices [4] with an organ conformed complex shapes made of functionally gradient materials are typically desired.

In our earlier work [1], we developed a new toolpath methodology to build up tissue scaffolds with controlled porosity architecture. Offsetting technique was used to create multi-regions with different porosity requirements. Thus, each region constituted various numbers of filaments with different inter-distance in between [5] in Cartesian coordinates. A toolpath optimization technique was developed to minimize fluid flow congestion with continuous toolpath deposition [6] to avoid start and stop during material deposition. However, imposition of any hollowed feature in a tissue model such as aorta brings jumps (starts and stops) during deposition process and developed modeled showed failures locally.

In Ozbolat and Koc [7], we proposed a toolpath planning for solid freeform deposition in 3D engineered wound devices. A 3D blending process is developed to generate functionally gradient uniform regions with different biomaterial and loaded biomolecule concentrations. Toolpath planning was developed in Cartesian coordinates is however no more than an approximation while blending direction is independent of toolpath deposition direction. As shown in Fig. 1(a), toolpath follows Cartesian coordinates and it does not follow blending directions between two features as illustrated in Fig. 1(b). Thus, the toolpath in Fig. 1(a) does not capture the geometry and smaller raster size with smaller gap between adjacent rasters is required for improved accuracy. Moreover, jumps or motion without deposition is highly substantial due to the nature of the toolpath that is independent of feature geometry. Almost all of the toolpath planning in the literature propose similar deposition in the Cartesian coordinates imposing hollowed shapes [8] in object architecture however triggers the severity of the approximation error. Qiu and Langara [9] addressed this problem; however, the developed methodology was no more than improvement in space filling. In that work, they minimized the gap by introducing adaptive roadwidth toolpath generation method but imposing several hollowed shapes brings too many starts and stops during deposition. Deposition process again follows Cartesian coordinates that is independent of hollowed feature geometry.

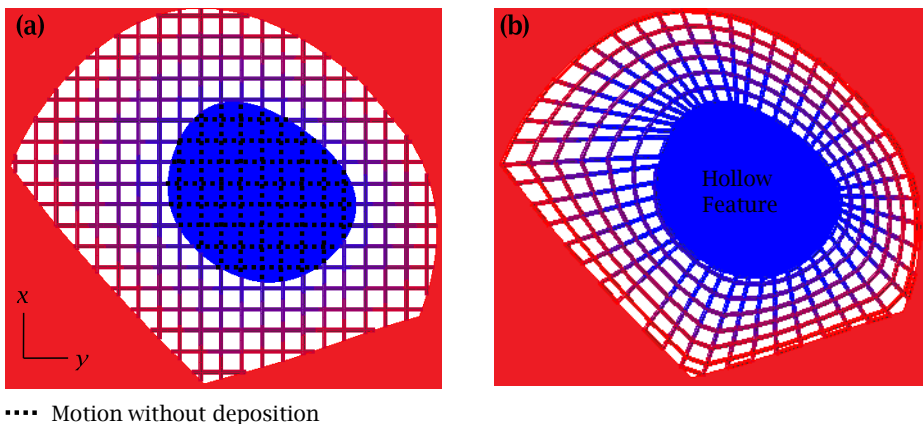


Fig. 1: (a) Shortcomings of traditional toolpath in Cartesian coordinates such as material blending direction is independent from the deposition direction and jumps due to hollow feature, and (b) a new toolpath strategy overcoming these shortcomings

Xu and Shaw [10] introduced design of functionally graded materials with internal holes for solid freeform fabrication. They proposed equal distance offset approach to generate gradients from bounding curve to the internal curves with identical material properties in a 2D slice of a 3D object. Although material properties vary smoothly for a slice with single internal curve, multiple internal curves generates non-smooth gradients when offset curves approach multiple internal curves, due to the nature of offset curves. Kim *et al* [11] addressed toolpath planning shortcomings with internal hollow shape for ablation processes such as lasers and electric power processes. The layer was decomposed into subregions by minimizing dwell time and energy requirement. Choi and Cheung [12] introduced virtual prototyping of multi-material deposition through multiple nozzles. In this paper, zigzag toolpath is used to fill contours; one embedded into the other defined by parent-child relations and a new methodology was developed to avoid nozzle collision. W. M. Zhu and K. M. Yu [13] proposed a dixel based slicing of objects with assemblies with multi-material properties, but it created objects with no more than single discrete entities. Chiu [14] designed and fabricated hollowed objects, in which voids were represented as repeating Voxel elements, with a toolpath generated using ray representation. Ray-representation of objects such as honeycomb and square shape objects however brings tremendous start and stops during fabrication process. During solid freeform fabrication, material deposition may start and stop periodically depending on the internal architecture. Starts and stops degenerate uniformity of the deposited material shape and need to be avoided [1].

In this paper, we propose a new toolpath planning scheme for hollowed scaffolds with multiple material voids based on our recent work in heterogeneous object modeling [15]. Generated ruled surface [15] is used to design the toolpath by eliminating abovementioned short comings of traditional

and recent approaches in hollowed object prototyping. Ruling lines, which are called material changing lines in this study, are reprocessed through matching and relaxation operations. A new layer-by-layer deposition process is developed in two consecutive layers: The first layer with material changing line based zigzag pattern and the next layer with spiral pattern deposition.

2 GEOMETRIC MODELING

In our recent work [15], we proposed a method to create ruled surface for hollowed objects with multiple internal features (See Fig. 2(a)) and proposed a novel multi-material blending approach in heterogeneous object modeling. In [15], the Voronoi diagram was generated and a number of Voronoi cells were obtained for each individual internal feature as shown in Fig. 2(b). Next, curve matching was developed to insert optimum ruling lines for each unit cell. Then, a ruling line alignment technique was developed to align ruling lines inserted between the external curve and the Voronoi while material properties change from external curve to the internal hollowed features.

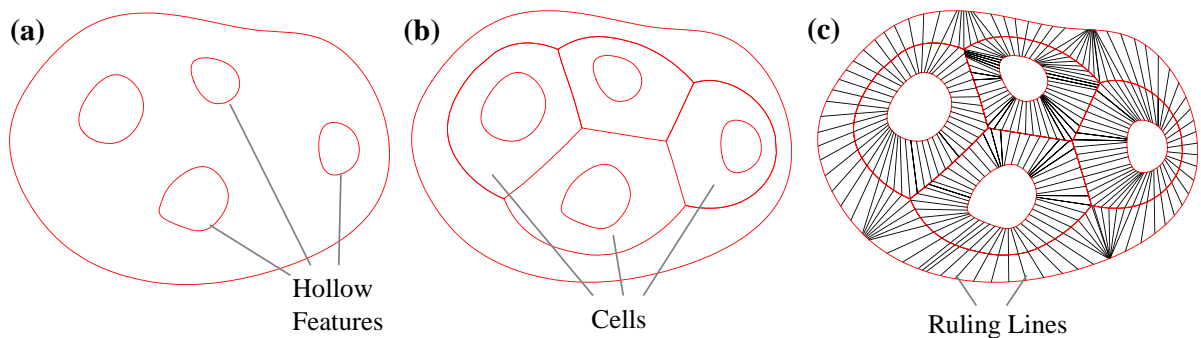


Fig. 2: Ruled Surface Construction: (a) A slice with multiple hollow shapes is decomposed to (b) cells using the Voronoi diagram and (c) curve matching and ruling line alignment techniques have been used to create ruled surface.

Due to shortcomings of toolpath planning in Cartesian coordinates, we propose a new toolpath planning scheme for objects with multiple hollow features through material blending direction. Ruling lines as shown in Fig. 2(c) [15] are proposed to be entities between two material features that plans the toolpath. These entities in this paper are called as 'Material Changing Lines' and material composition alters in material changing lines' orientation direction gradually between two features.

In this work, toolpath planning through material changing lines (MCLs) creates over-deposition and self-intersections on bisector of two internal features as shown in Fig. 2(c). In order to overcome this problem, a material changing line matching technique is proposed for minimum over-deposition or stop and starts during free-form deposition.

2.1 Matching of Material Changing Lines

Material changing lines between adjacent cells in our earlier work [15] were inserted independent of MCLs in adjacent cells while impact of their connectivity was not critical. However, this brings discontinuities between MCLs that create an important shortcoming in toolpath planning. Fig. 3(a) highlights the discontinuities between MCLs on adjacent cells. During toolpath planning, toolpath needs to be continuous that necessitates the connection of MCLs between two adjacent cells. Without matching of MCLs, toolpath follows the Voronoi diagram to travel through unconnected MCLs. This however triggers over-deposition on the Voronoi.

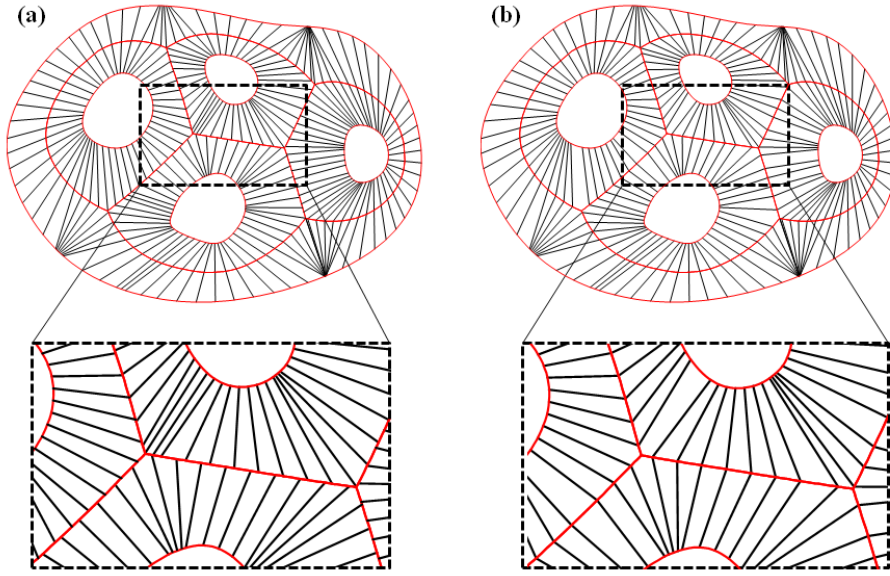


Fig. 3: Matching of material changing lines between cells: (a) Unmatched material changing lines with discontinuities between material changing lines of adjacent cells and (b) matching of material changing lines for continuous toolpath planning

Thus, a material changing line matching technique is proposed to connect dispatched MCLs on adjacent cells. For each bisector between two cells, MCLs are traced and MCLs are ranked based on their priority. Two conditions can be used to express the priority analytically:

- i. The normal vectors of connection points on two curves needs to collinear for perfect matching. This enables smooth transitions of material composition through the MCLs between two material properties.
- ii. In order to reduce fabrication time, length of MCLs should be minimized.

Using above conditions, an objective function can be introduced as:

$$f(\mathbf{p}_i^k; \mathbf{q}_r^s) = \frac{\langle \vec{\mathbf{N}}(\mathbf{p}_i^k), \vec{\mathbf{N}}(\mathbf{q}_r^s) \rangle^{w_n}}{\left| \mathbf{p}_i^k - \mathbf{q}_r^s \right|^{w_d}} \quad (2.1)$$

Where $\mathbf{P}^k = \mathbf{p}_i^k$ is a point set, sampled from bisector $B_k(u)$ on the Voronoi diagram and $\vec{\mathbf{N}}(\mathbf{p}_i^k)$ is the corresponding normal vector for $\exists \mathbf{p}_i^k : \mathbf{p}_i^k \in \mathbf{P}$ as shown in Fig. 4. In Equation (2.1), \mathbf{q}_r^s is r^{th} point sampled from hollowing curve HC_s . Point sampling in each curve is performed over its parametric domain such as:

$$\begin{aligned} \mathbf{P} &= \mathbf{p}_i^k \quad_{i=1, \dots, I}; \text{ where } \mathbf{p}_i^k = B_k(u_i); u_i \in [u_{p_1}, u_{h_1}]; \\ &u_i < u_{i+1}; u_0 < u_{p_1}; u_1 < u_{h_1} \\ \mathbf{p}_0^k &= B_k(u_0) = B_k(u_{p_1}) \text{ and } \mathbf{p}_1^k = B_k(u_1) = B_k(u_{h_1}) \end{aligned} \quad (2.2)$$

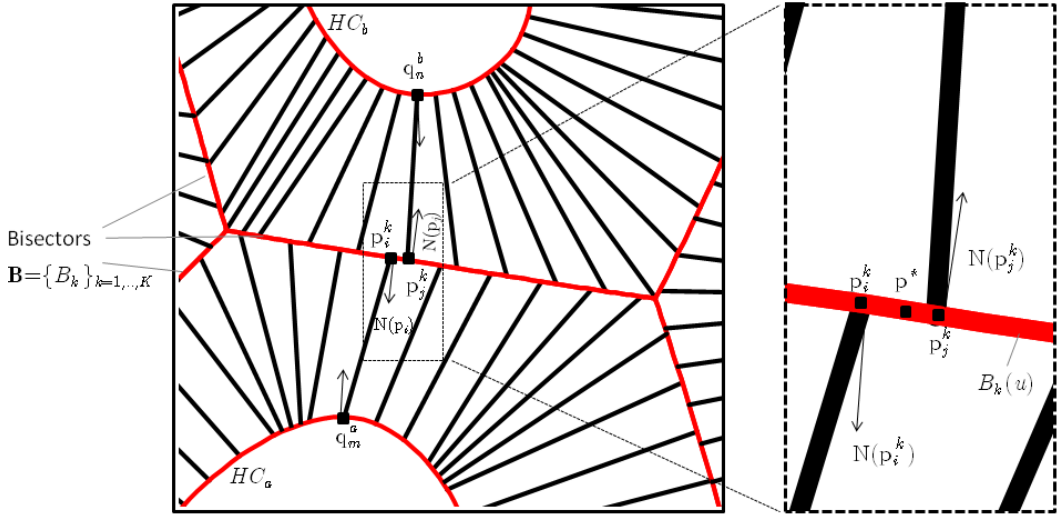


Fig. 4: Matching between material changing lines based on an objective function

A greedy heuristic optimization approach developed in our earlier work [17] is applied to perform MCL matching. The approach begins with searching a material changing line with maximum objective function called $\max\{MCL\}$. Then, proximity of other MCLs from the adjacent cell is calculated on the bisector curve. The closest one is chosen and corresponding objective function is calculated. A proximity upper bound is introduced as a user inputted value so that if the distance of the candidate MCL (CMCL) exceeds the upper bound, then it is not considered as feasible. This will prevent connection of CMCL that is considerably apart from $\max\{MCL\}$ although it is the closest among other CMCLs. In this case, $\max\{MCL\}$ is deleted out while there is no feasible candidate for matching. Then intersection points of two MCLs on the bisector curve is matched by obtaining a weighted point on the bisector curve between two intersection points based on objective function values of two MCLs. Next, weighted point is calculated as:

$$\mathbf{p}^*(u^*) = \frac{\mathbf{p}_i^k(u_i)f(\mathbf{p}_i^k, \mathbf{q}_m^a) + \mathbf{p}_j^k(u_j)f(\mathbf{p}_j^k, \mathbf{q}_n^b)}{f(\mathbf{p}_i^k, \mathbf{q}_m^a) + f(\mathbf{p}_j^k, \mathbf{q}_n^b)} \quad (2.3)$$

$$\mathbf{p}_i^k = B_k(u_i), \mathbf{p}_j^k = B_k(u_j), \mathbf{p}^* = B_k(u^*)$$

Two MCLs are then reconstructed and their intersection points with the bisector curve are shifted to the weighted point. This procedure is repeated until all MCLs on the bisector curve are matched with MCLs of the adjacent cell. Those that do not have a matching pair are removed and same technique is applied for each bisector curve. Fig. 3(b) illustrates the final result of matched MCLs. As a result, the toolpath can be constructed through each MCL continuously. Once it approaches the bisector curve, it directly proceeds with the matched pair and passes to the other cell. This eliminates over-deposition of material or self-intersection of toolpath on the bisector curve. The following algorithm is generated for MCL matching in a Voronoi cell:

Algorithm I: MCL Matching

Input: A set of available material changing lines $MCL = MCL_t \quad t=1, \dots, T$, upper distance bound δ

Output: A set of new material changing lines $nMCL = nMCL_v \quad v=1, \dots, V$

1. $\forall MCL_t$
2. Initialize $CMCL \rightarrow \emptyset; i \rightarrow 1;$
3. **For** $t=1$ to T

4. **If** $MCL_i \cap B_k(u) \neq \emptyset$ **then** $CMCL_i \rightarrow CMCL_i \cup MCL_i$;
5. Calculate objective function f_i using Equation (2.1);
6. $i \rightarrow i+1$;
7. **End If**
8. $I \rightarrow i$;
9. **End For**
10. Initialize $\max \rightarrow 0$;
11. **For** $i=1$ to I
12. **If** $f_i > \max$ **then** $\max \rightarrow f_i$; $temp \rightarrow i$;
13. **End If**
14. **End For**
15. Get $dist = \min |p_{temp}^k, p_j^k|$
16. **If** $dist < \delta$ **then** calculate p^* using Equation (2.3) and generate $nMCL_v = \overline{q_n^a, p^*} \cup \overline{p^*, q_n^b}$;
17. **Else Delete** MCL_{temp} ;
18. **End If**

2.2 Material Changing Line Relaxation

Perfect alignment of material changing lines enables a smooth transition of material properties between two features. Material changing lines that are closed to branch points cannot be aligned perfectly while they intersect each other. Hence, MCLs are added based on the MCL insertion technique that is introduced in our earlier work [15]. This enforces density of ruling lines over regions that are closed to branching points. Although this can be acceptable for modeling purposes, it brings an over-deposition problem in the fabrication process. Fig. 5(a) shows the over-deposition problem highlighted in a circle.

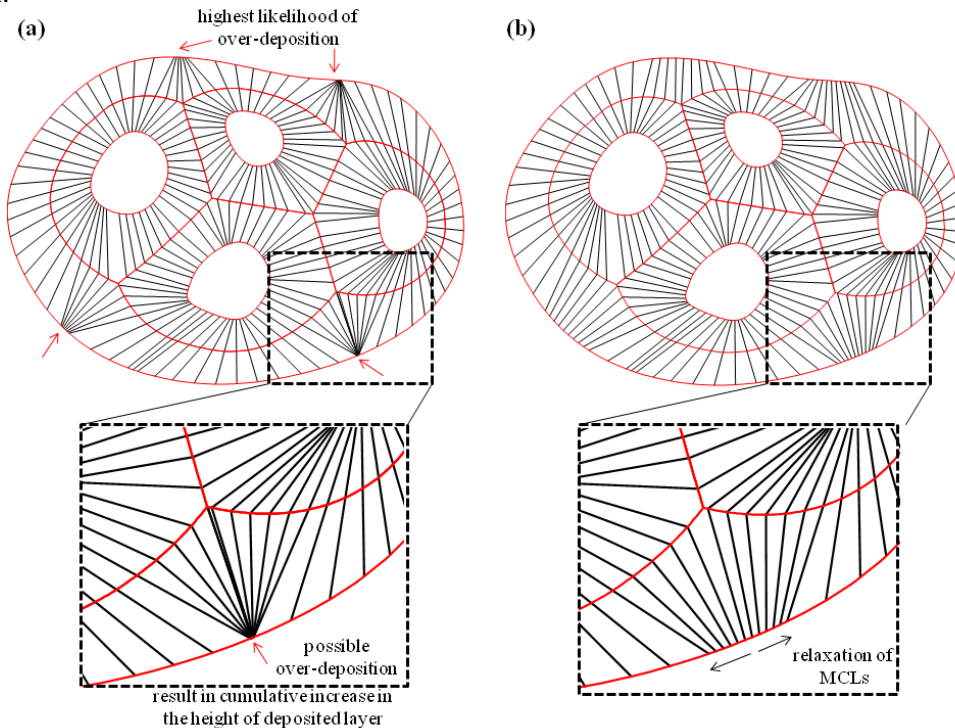


Fig. 5: MCL Relaxation Technique to alleviate over-deposition

Applying this procedure in toolpath planning however triggers over-deposition remarkably over regions that are closed to the branching points. This can be partially eliminated by increasing deposition speed or feedrate while approaching to these regions. In order to decrease the effect of over deposition considering the nonuniformity in these regions, a MCL relaxation methodology is developed. MCLs that are not aligned nearby the branching points are moved away from each other by dispersing them through the extra space. This extra space is created by shifting edge of closest aligned MCLs on the external curve through adjacent MCLs. This is followed by shifting the non-aligned MCLs through the shifted aligned lines with the same parametric distance in between. Hence, gap between MCL is enlarged and over-deposition can be alleviated relatively. Relaxation can be applied iteratively until all denser regions are eliminated depending on user inputted values. After the relaxations, MCLs can be used for toolpath modeling. Next section introduces the toolpath planning through MCLs' orientation direction.

2.3 Material Deposition through Material Changing Line Orientation Direction

The toolpath should be planned through inserted MCLs with minimum amount of over deposition, and start and stops. In this work, toolpath planning firstly crosshatches the region between the external material feature and internal material features. The material changing lines shown in Fig. 6(a) is used to generate the toolpath. The toolpath needs to start at a MCL just after one of the branching points while initialization of toolpath on another MCL brings jumps during deposition process. In addition, if the number of material changing line on the external material feature is odd, then toolpath should start from the external material feature; otherwise it should start from the internal material feature to eliminate any possible jumps. This enables completion of crosshatching at the internal material feature and transition of toolpath without any jumps through the inner regions. Fig. 6(b) highlights filling of MCLs between the external curve and internal curves, and the toolpath for this region is completed as illustrated in Fig. 6(c).

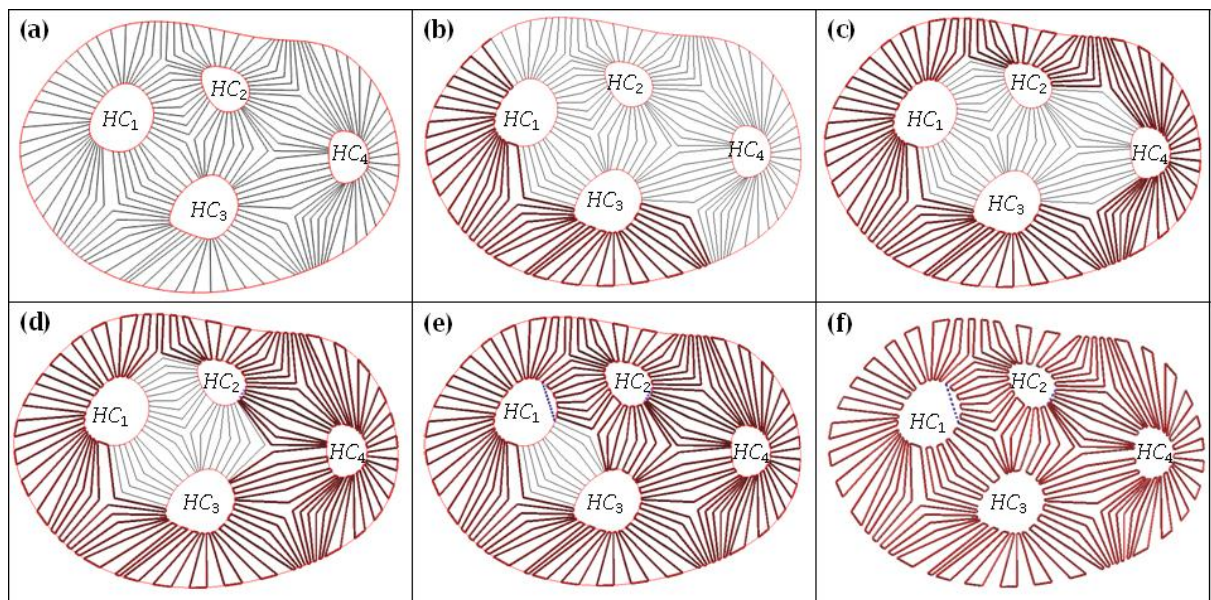


Fig. 6: Simulation of toolpath planning for the deposition through MCLs.

Once the external region is crosshatched, then toolpath proceeds with the internal region and fills the internal region until it crosses with filled region. Fig. 6(d) highlights the intermediate deposition in the internal region: first between HC_3 - HC_4 , and then between HC_2 - HC_4 . During crosshatching over the internal or external regions, toolpath selects the closest unoccupied point to move and it makes tracing over the corresponding MCL. Then, toolpath proceeds through MCLs between other internal material

feature couples as shown in Fig. 6(e). Toolpath traces MCLs between HC_2 - HC_3 , and then between HC_2 - HC_1 . Once closest point is in a direction that a jump is needed, the toolpath then continuous with a jump to that point as shown in Fig. 6(e) with blue dash lines (to trace MCLs between HC_1 - HC_3 in this example). These jumps in this study are unavoidable during internal region deposition. However total jump distances can be minimized by selecting the shortest unoccupied MCLs during jumps. Finally, the toolpath can be obtained as shown in Fig. 6(f). In this section, MCL based zigzag toolpath plan is proposed. Next section introduces a deposition pattern for the consecutive layer in layer-by-layer manufacturing.

2.4 Spiral Pattern Toolpath

Lay-down pattern style, i.e. in general 0-90° orientation, has been widely used in layer-by-layer manufacturing to build objects in vertical direction, in which each layer supports the next one [5]. In order to support the zigzag pattern discussed in Section 2.3, a spiral toolpath plan is proposed for the next layer, in which spiral toolpath is closely perpendicular to MCLs at the support point. The advantages of the spiral toolpath are as follows:

- Spiral toolpath enables a continuous deposition through a hollow feature compared to conventional zigzag based space filling technique;
- A smooth transition from one material composition property to another one can easily be generated;

During the insertion of MCLs, imposed visibility and non-intersection constraints enables nonintersecting MCLs that was extensively discussed in our earlier study [15] (Extreme cases were also tested and zero degeneration was achieved in that study). A piecewise spiral curve $S(t) = \text{MCL}_v(u)$ is generated as a dependent of MCLs, where u is a parametric variable in MCL orientation direction and controls the material composition. v is another parametric variable through the sampled points on the hollow feature (See Fig. 7). In this paper, u is defined as $u = f(v)$, where f is the spiral path control function that can be inputted by the user and controls the shape and the number of contours in the spiral.

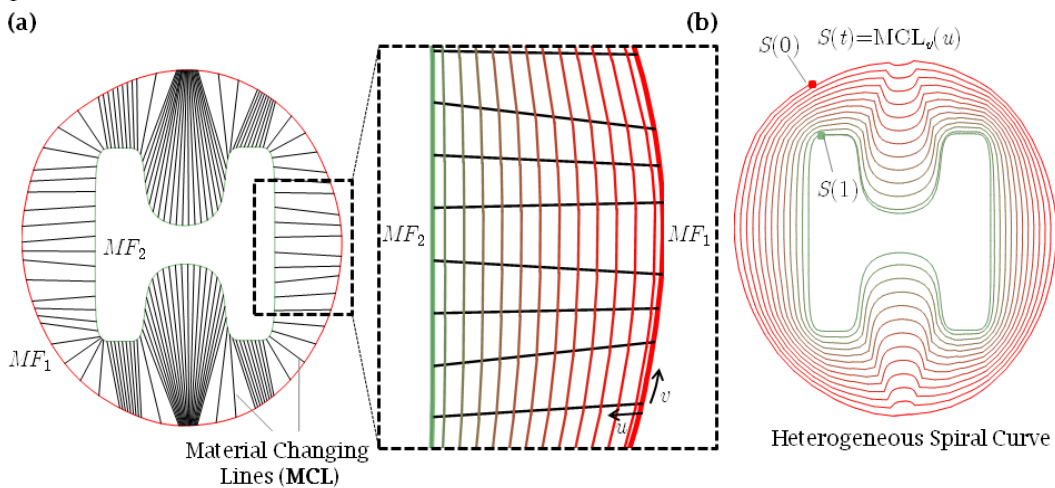


Fig. 7: Heterogeneous spiral toolpath

Increasing number of MCLs improves the accuracy of the spiral curve however toolpath planning through MCL orientation direction generates over deposition due to the increasing density. This technique is applied for each Voronoi cells shown in Fig. 2 to generate spiral toolpath for objects with multiple hollowed features. Jumps during shifting from one Voronoi cell to another is however observable in some circumstances and developing a toolpath with zero start and stop might be a promising future direction. In the next section, implementation and illustrative examples are presented.

3 IMPLEMENTATION AND EXAMPLES

The proposed methodologies are coded in VB based Rhinoscript and examples are generated in Rhinoceros 4.0 software [18]. Three examples of multi-material toolpath are generated by assigning different material properties represented by different values in RGB color space as shown in Fig. 8-10. Examples are generated on a computer with Intel Pentium 2 GHz processor and 1GB of RAM. A linear function $f(v) = v$ is used for the generated examples. Examples with four, two and three hollow features are presented in Fig. 8, Fig. 9 and Fig. 10 respectively. Fig. 8(a)-10(a) illustrate material composition requirement for a slice from each object with several internal hollow features, each dominated with a distinct material composition from the material domain $M = M_i \quad i=1,\dots,l$. MCL based zigzag patterns are shown for three different examples in Fig. 8(b)-10(b). Material composition of the zigzag pattern is mapped based on the parametric distance interpolation of two features. Fig. 8(c)-10(c) demonstrate spiral patterns for three cases and combined toolpath for consecutive layers are presented in Fig. 8(d)-10(d) and 8(e)-10(e).

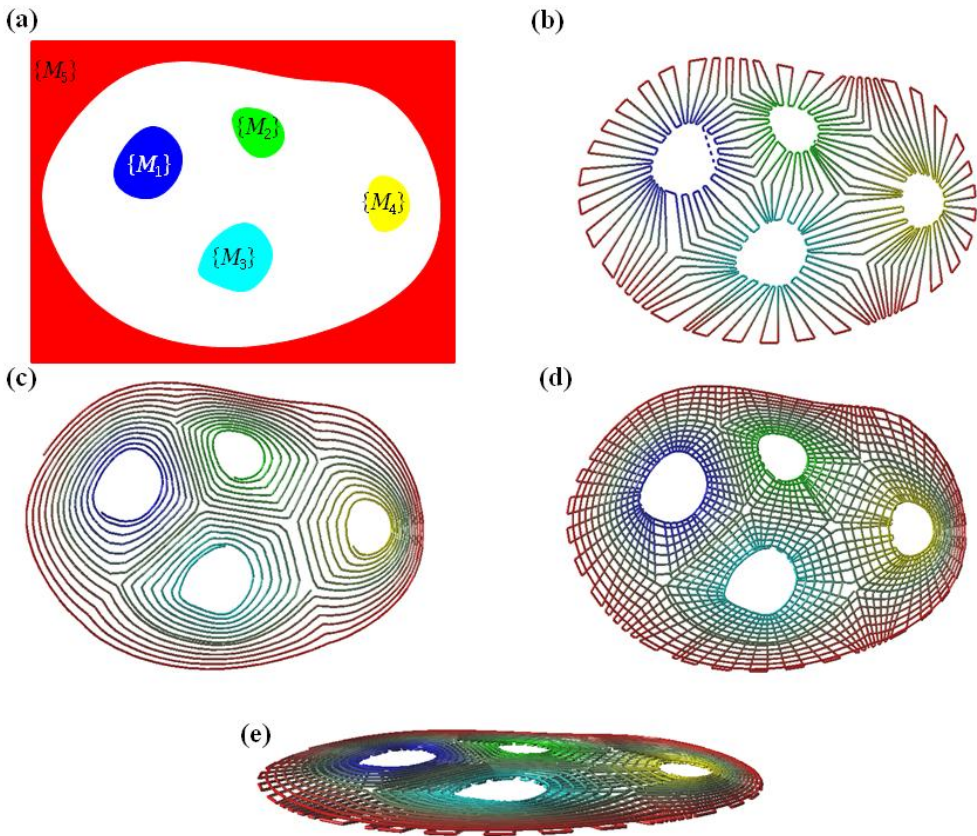


Fig. 8: Example of a multi-material toolpath with 4 hollow features

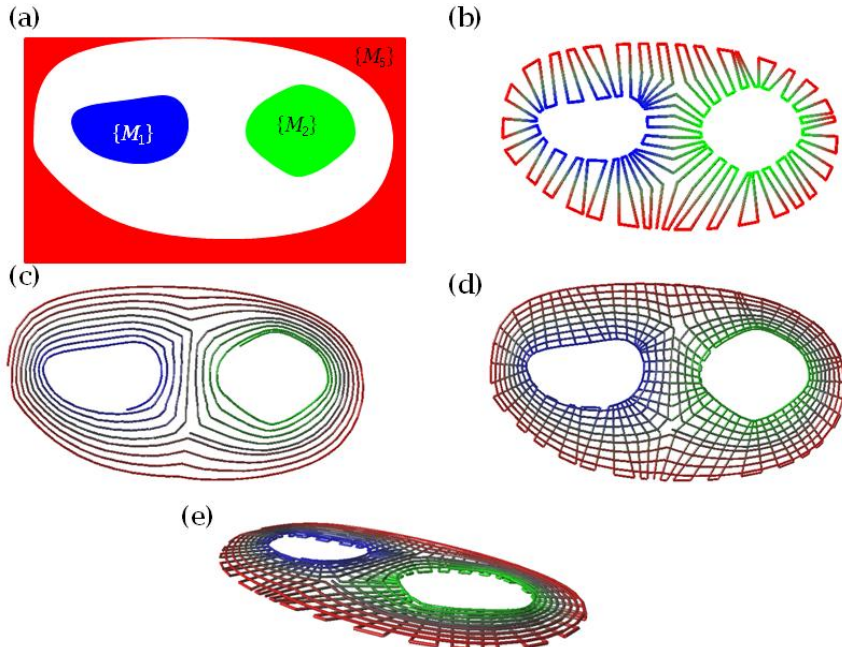


Fig. 9: Example of a multi-material toolpath with 2 hollow features

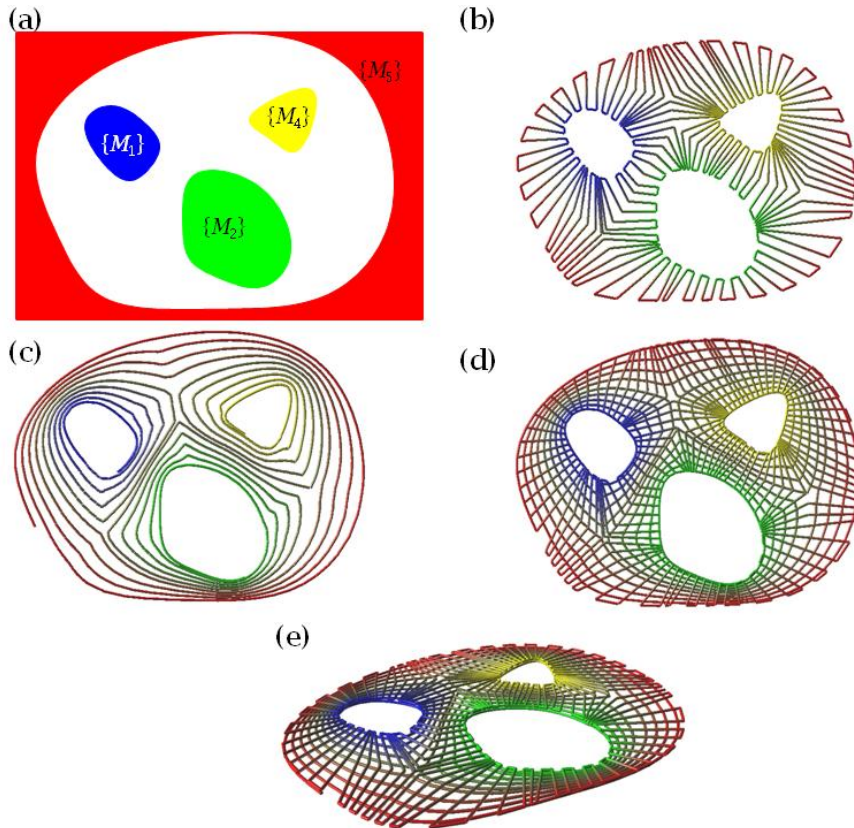


Fig. 10: Example of a multi-material toolpath with 3 hollow features

4 CONCLUSION

In this paper, a new toolpath planning scheme is proposed for heterogeneous tissue scaffold modeling and fabrication. Material changing lines developed in our earlier work has been post processed through few steps such as material changing line matching and material changing line relaxation with reduced number of start and stops, and hence lessened effect of over-deposition. Layer-by-layer deposition process in this work is progressed in two steps: The first layer with zigzag pattern through material changing lines and the second layer with spiral pattern. Material composition properties are mapped based on the parametric distance from the hollow features.

REFERENCES

- [1] Khoda, A.; Ozbolat, I.T.; Koc, B.: Engineered Tissue Scaffolds with variational porosity architecture, ASME Transactions, Journal of Biomechanical Engineering, 133(1), 2011, 011011(1)-011011(12). DOI:10.1115/1.4002933
- [2] Ozbolat, I.T.; Marchany, M.; Bright, F.V.; Cartwright, A.N.; Gardella, J.A.; Hard, R.; Hicks, W.L.; Koc, B.: Feature Based Bio-Modeling of Micro-patterned Structures for Tissue Engineering, Computer-Aided Design and Applications, 6(5), 2009, 661-671. DOI:10.3722/cadaps.2009.661-671
- [3] Ozbolat, I.T.; Marchany, M.; Bright, F.V.; Cartwright, A.N.; Gardella, J.A.; Hard, R.; Hicks, W.L.; Koc, B.: Computer-aided Bio-modeling of Micro-patterned Structures for Tissue Engineering in: Industrial Engineering Research Conference, IERC 2009, Miami, FL, 2009.
- [4] Ozbolat, I.T.; Koc, B.: Modeling of Spatially Controlled Biomolecules in Three-dimensional Porous Alginate Structures ASME transactions, Journal of Medical Devices, 4(4), 2010, 041003(1)-041003(11). DOI: 10.1115/1.4002612
- [5] Ozbolat, I.T.; Khoda, A.; Koc, B.: Geometric Modeling of Complex Tissue Engineering Scaffolds with Controlled Porosity Distribution, in: Industrial Engineering Research Conference, Miami, FL, 2009.
- [6] Ozbolat, I.T.; Khoda, A.; Koc, B.: Toolpath Optimization in Solid Freeform Design and Fabrication, in: Industrial Engineering Research Conference Cancun, Mexico, 2010.
- [7] Ozbolat, I.T.; Koc, B.: Multi-function based 3D Heterogeneous Wound Scaffolds for Improved Wound Healing, Computer-Aided Design and Application, 8(1), 2011, 43-57. DOI: 10.3722/cadaps.2011.43-57
- [8] Cai, D.; Shi, Y.; Zhang, L.; Huang, S.: The two-dimension hollowing algorithm for rapid prototyping technology, Int J Adv Manuf Technol, 33, 2007, 738-745.
- [9] Qui, D.; Langrana, N.A.: Void eliminating toolpath for extrusion-based multi-material layered manufacturing, Rapid Prototyping Journal, 8, 2002, 38-45. DOI: 10.1108/13552540210413293
- [10] Xu, A.; Shaw, L.L.: Equal distance offset approach to representing and process planning for solid freeform fabrication of functionally graded materials, Computer-Aided Design, 37, 2005, 1308-1318. DOI: 10.1016/j.cad.2005.01.005
- [11] Kim, H.C.; Lee, S.H.; Yang, D.Y.: Toolpath planning algorithm for the ablation process using energy sources, Computer-Aided Design, 41, 2009, 59-64. DOI: 10.1016/j.cad.2008.12.005
- [12] Choi, S.H.; Zhu, W.K.: A dynamic priority-based approach to concurrent toolpath planning for multi-material layered manufacturing, Computer-Aided Design, 42, 2010, 1095-1107. DOI: 10.1016/j.cad.2010.07.004
- [13] Zhu, W.M.; Yu, K.M.: Dixel-Based Direct Slicing of Multi-Material Assemblies, Int J Adv Manuf Technol, 18, 2001, 285-302.
- [14] Chiu, W.K.; Tan, S.T.: Using dexels to make hollow models for rapid prototyping, Computer-aided Design, 30, 1998, 539-547. DOI: 10.1016/S0010-4485(98)00008-6
- [15] Ozbolat, I.T.; Koc, B.: Multi-target Blending for Heterogenous Object Modeling, Computer-Aided Design, 2010, (Under 2nd Review).
- [16] Samanta, K.; Koc, B.: Optimum matching of geometric features for material metamorphosis in heterogeneous object modeling, Computer-Aided Design and Applications, 4, 2007, 57-66.
- [17] Samanta, K.; Koc, B.: "Feature-Based Material Blending for Heterogeneous Object Modeling," Heterogeneous Objects Modeling and Applications, A. Pasko, V. Adzhiev, P. Comninos, Eds., 2008, 142-167.
- [18] RobertMcNeel&Associates, Rhinoceros 4.0, in, Seattle, 2007.